

## Infrared Diode Laser Spectra of the $\Delta v = 1$ Band of AlF and the $\Delta v = 2$ Band of KF

A. G. MAKI AND F. J. LOVAS

*Molecular Spectroscopy Division, National Bureau of Standards, Washington, D. C. 20234*

High-resolution diode laser spectra of AlF and of KF were measured between 827 and 855  $\text{cm}^{-1}$ . Measurements were made on the  $v = 1-0$ ,  $2-1$ , and  $3-2$  transitions of AlF at temperatures between 1000 and 1190 K. The band centers were determined to be at  $792.6882 \pm 0.0004 \text{ cm}^{-1}$ ,  $783.1633 \pm 0.0004 \text{ cm}^{-1}$ , and  $773.7534 \pm 0.0007 \text{ cm}^{-1}$ , respectively. For KF, temperatures between 1150 and 1250 K were used to measure the  $v = 2-0$ ,  $3-1$ , and  $4-2$  transitions for which the band centers were determined to be at  $837.9702 \pm 0.0003 \text{ cm}^{-1}$ ,  $828.3966 \pm 0.0003 \text{ cm}^{-1}$ , and  $818.9350 \pm 0.0005 \text{ cm}^{-1}$ , respectively. These infrared measurements were combined with microwave measurements, reported by others, to obtain new Dunham constants for AlF and for KF. The values for  $\omega_e$ ,  $B_e$ , and the Dunham  $a_i$  potential constants were obtained directly from the observed transitions by means of a nonlinear least-squares analysis.

### I. INTRODUCTION

At high temperatures aluminum monofluoride (AlF) is easily produced in the gas phase and has been the subject of numerous visible and microwave studies (1-7). AlF also has been observed to give stimulated infrared emission (laser action) in an exploding wire experiment (8). However, in the infrared region only the matrix isolation spectrum of AlF has been studied in detail (9). In this paper we report the first observation of the resolved infrared gas phase spectrum of AlF in the  $^1\Sigma^+$  ground electronic state.

The potassium fluoride monomer molecule (KF) is also easily produced in the gas phase and both microwave (10-12) and low-resolution infrared measurements (13-14) have been reported for KF. A matrix isolation study also has been made on the infrared spectrum of KF in an argon matrix (15). Prior to the present work, the best information on the vibrational energy levels for KF came from the Dunham constants calculated by Veazey and Gordy (11) from microwave measurements of rotational transitions.

Previous infrared measurements had concentrated on observing the fundamental band of KF since it is more intense than the first or higher overtones. In the present paper the gas-phase spectrum of the first overtone of KF was measured rather than the fundamental since the first overtone is the only KF band within the range of our diode laser system.

### II. EXPERIMENTAL DETAILS

The AlF was produced in the absorption cell in a tube oven by heating a stoichiometric mixture of Al powder and  $\text{AlF}_3$ . The high temperature absorption cell

was a 28-mm-o.d., 75-cm-long alumina tube identical to that used to measure SiO (16). Argon gas at a pressure of about 5 Torr (700 Pa) was used as a buffer. The hot zone of the tube oven was 36 cm long. The strongest AlF lines were first observed at temperatures around 1000 K but most of the measurements were made at temperatures between 1090 and 1190 K (as measured with a Pt to Pt-10% Rh thermocouple placed at the center of the oven).

The KF was vaporized from the crystalline powder by heating in a 28-mm-o.d., 90-cm-long stainless-steel absorption tube that was placed in a 36-cm-long tube oven. Sodium chloride windows were attached to the ends of the stainless-steel tube and were far enough outside the oven to be kept at room temperature. A buffer gas of 10 to 15 Torr (1300 to 2000 Pa) of argon was used to prevent rapid diffusion of the KF vapor to the cool portions of the absorption tube. The KF spectrum was measured at a temperature that varied from 1150 to 1250 K. With a single charge of about 7 grams of KF, it was possible to measure spectra for at least four hours. The absorption tube appeared to act like a heat pipe by allowing the condensed liquid KF to flow from the cooler ends back into the hot zone.

Both the AlF and KF spectra were measured with a single tunable diode laser element which emitted laser radiation between 827 and 880  $\text{cm}^{-1}$  although the spectral coverage was far from complete within that interval. The spectra were calibrated by means of OCS absorption lines. The OCS frequencies were calculated from the constants given in Refs. (17) and (18) and are believed to be accurate to  $\pm 2$  MHz or better. The individual AlF and KF line frequency measurements were estimated to be accurate to within  $\pm 15$  MHz on the average. The measurement technique was the same as that described in Ref. (19) although the temperature regulation of the germanium etalon was improved for the KF measurements.

### III. ASSIGNMENT AND PRELIMINARY ANALYSIS OF THE DATA

#### A. The AlF Spectrum

By using the Dunham constants given by Wyse *et al.* (5) it was possible to calculate the infrared spectrum of AlF with sufficient accuracy to readily identify the first AlF transitions that were measured. The new measurements were then combined with the microwave measurements in a least-squares analysis which gave an improved estimate of the Dunham constants. The measured transition wavenumbers and their assignments are given in Table I. No absorption features were observed that could not be assigned to AlF.

The infrared measurements given in Table I were combined with the microwave measurements given in Refs. (5-7) in a preliminary least-squares analysis based on the usual Dunham equation (20)

$$\nu_{\text{obs}} = \sum_{ij} Y_{ij} \{ [v' + 1/2]^i [J'(J' + 1)]^j - [v'' + 1/2]^i [J''(J'' + 1)]^j \}. \quad (1)$$

The low  $J$  microwave transitions reported in the literature included contributions from the nuclear quadrupole moment of the aluminum. This hyperfine structure was removed by using the quadrupole coupling constants given in Refs. (6) and (7) and the hypothetical center frequency was used in the least-squares analysis.

TABLE I  
Observed  $\Delta v = 1$  Transitions of Aluminum Monofluoride (AlF)

$v' - v''$	ROT. TRANS.	OBSERVED(UNC) <sup>a</sup> ( $\text{cm}^{-1}$ ) <sup>b</sup>	$0 - c^c$ $\times 10^5$ ( $\text{cm}^{-1}$ )
1 - 0	R(39)	828.30696(40)	-14
1 - 0	R(40)	828.98049(133)	-62
1 - 0	R(41)	829.64410(133)	-12
1 - 0	R(47)	833.39271(40)	-14
1 - 0	R(53)	836.74356(40)	5
1 - 0	R(54)	837.26379(250)	87
1 - 0	R(55)	837.72224(83)	113
1 - 0	R(56)	838.26805(40)	0
1 - 0	R(68)	843.34666(83)	3
1 - 0	R(70)	844.03244(40)	-23
1 - 0	R(86)	847.83954(40)	1
1 - 0	R(87)	847.97750(40)	47
1 - 0	R(88)	848.10242(40)	-17
1 - 0	R(91)	848.40747(40)	8
1 - 0	R(92)	848.48469(40)	-27
1 - 0	R(93)	848.55080(40)	32
1 - 0	R(103)	848.53882(80)	53
2 - 1	R(54)	827.30313(67)	-12
2 - 1	R(56)	828.29705(40)	25
2 - 1	R(58)	829.24548(133)	-14
2 - 1	R(59)	829.70370(133)	50
2 - 1	R(66)	832.59022(40)	20
2 - 1	R(68)	833.31202(40)	-49
2 - 1	R(80)	836.67935(40)	-34
2 - 1	R(86)	837.73354(67)	16
2 - 1	R(87)	837.86870(167)	101
2 - 1	R(88)	837.98979(40)	-36
2 - 1	R(89)	838.10067(40)	-6
2 - 1	R(90)	838.19927(40)	-15
2 - 1	R(91)	838.28597(40)	-22
2 - 1	R(92)	838.36098(40)	-3
2 - 1	R(93)	838.42403(40)	15
2 - 1	R(94)	838.47446(40)	-31
2 - 1	R(95)	838.51379(40)	13
2 - 1	R(100)	838.52723(40)	-12
2 - 1	R(101)	838.49381(40)	0
2 - 1	R(102)	838.44811(40)	0
2 - 1	R(103)	838.39060(40)	35
2 - 1	R(104)	838.32009(40)	-12
2 - 1	R(105)	838.23810(60)	13
2 - 1	R(106)	838.14353(40)	4
2 - 1	R(107)	838.03706(40)	28
2 - 1	R(109)	837.78745(100)	91
3 - 2	R(83)	827.28642(40)	-1
3 - 2	R(84)	827.45317(40)	30
3 - 2	R(91)	828.28902(40)	0
3 - 2	R(92)	828.36143(40)	19
3 - 2	R(94)	828.46931(133)	-74
3 - 2	R(95)	828.50713(67)	53
3 - 2	R(96)	828.53142(40)	19
3 - 2	R(97)	828.54386(40)	-5
3 - 2	R(103)	828.36730(40)	-60

<sup>a</sup> The estimated uncertainties in the last digits of the measured values are given in parentheses following each value for the observed wavenumbers.

<sup>b</sup> To convert to frequency units use the speed of light:  $c = 299792.458 \text{ km/s}$ .

<sup>c</sup> The last column gives the differences between the observed wavenumbers and the wavenumbers calculated using the Dunham potential constants given in Table III.

Each datum used in the analysis was weighted by the inverse square of its estimated uncertainty. The constants resulting from this analysis are given in the first column of Table II.

TABLE II  
Dunham Rovibrational Constants for AIF

	This work Fit of $Y_{ij}$	This work <sup>a</sup> Fit of $a_i$	Wyse et al. Ref. (5)
$Y_{10}(\text{cm}^{-1})^b$	802.32430(148) <sup>c</sup>	802.32497(129)	802.85(25)
$Y_{20}(\text{cm}^{-1})^b$	-4.849448(904)	-4.850283(678)	-4.86(6)
$Y_{30}(\text{cm}^{-1})^b$	0.019312(157)	0.0197584(861)	-
$Y_{40}(\text{cm}^{-1})^b$	-	-0.0000748(148)	-
$Y_{01}(\text{MHz})$	16562.93599(452)	16562.93824(305)	16562.930(6)
$Y_{11}(\text{MHz})$	-149.42811(742)	-149.42104(579)	-149.420(9)
$Y_{21}(\text{kHz})$	517.86(372)	514.88(353)	515.(4)
$Y_{31}(\text{kHz})$	0.992(533)	1.298(561)	1.4(6)
$Y_{02}(\text{kHz})$	-31.3778(127)	-31.414386(91)	-31.37(2)
$Y_{12}(\text{Hz})$	50.981(866)	52.468(197)	46.(14)
$Y_{22}(\text{Hz})$	2.065(111)	2.2281(563)	-
$Y_{03}(\text{mHz})$	$[-10.9]^d$	-10.93320(478)	-
$Y_{13}(\text{mHz})$	0.3610(417)	0.3197(129)	-
$Y_{04}(\mu\text{Hz})$	-	-0.037943(88)	-
rms dev. of infrared measurements	0.00037 $\text{cm}^{-1}$	0.00039 $\text{cm}^{-1}$	-

<sup>a</sup> Calculated from the  $a_i$  values given in Table III.

<sup>b</sup> To convert from wavenumber units to frequency units use the velocity of light,  $c=299792.458$  km/s.

<sup>c</sup> The uncertainty in the last digits (twice the estimated standard error) is given in parentheses following each value.

<sup>d</sup> The constant enclosed in square brackets was fixed at the value calculated from the  $a_i$  values given in Table III.

The microwave measurements used in this analysis cover a wide range of  $J$  values,  $J = 0$  to  $J = 14$ , and vibrational states,  $v = 0$  to  $v = 4$ . Because of the low-frequency limit on the tuning range of the diode laser used for this work, the infrared measurements do not include the  $P$  branch or band center regions, but do include very high  $J$   $R$ -branch transitions, extending beyond the  $R(98)$  bandhead for the three vibrational transitions that were measurable. In order to fit this wide range of data, 11 Dunham constants were needed.

It is surprising that the value of  $Y_{13}$  was determinable although the value of  $Y_{03}$  was not. This may be partly due to the sensitivity of infrared measurements to the vibrational dependence of rotational constants rather than to the rotational constants themselves. For this analysis, it was necessary to calculate the value of  $Y_{03}$ . The value of  $Y_{03}$  used in the final fit was calculated from the Dunham potential constants given in Table III and obtained from the nonlinear least-squares fit described below.

TABLE III  
Dunham Potential Constants Determined for AlF and KF

	AlF	KF
$\omega_e$ (MHz)	24053108.3(410) <sup>a</sup>	12779014.6(158)
$B_e$ (MHz)	16562.93001(274)	8392.29358(253)
$a_1$	-3.1834959(813)	-3.116761(212)
$a_2$	6.815735(629)	6.30754(236)
$a_3$	-11.5792(184)	-9.3631(185)
$a_4$	16.630(161)	9.626(399)
$a_5$	-22.514(454)	-5.13(222)
$a_6$	29.89(933)	-

<sup>a</sup> The uncertainty in the last digits (twice the estimated standard error) is given in parentheses following each value.

### B. The KF Spectrum

The observed KF lines were easily assigned by means of simulated spectra calculated using the Dunham constants given by Veazey and Gordy (11). Because of the limited spectral coverage available to us, only three vibrational transitions could be observed,  $v = 2-0$ ,  $v = 3-1$ , and  $v = 4-2$ . For all three, *R*-branch lines were measured through the bandhead at *R*(57) and up to *J* values that ranged from 75 to 103 for the different bands. Figure 1 shows the spectrum in the region of the *R*-branch bandhead for the  $v = 4-2$  transition. Only spectral features for the <sup>39</sup>K<sup>19</sup>F isotopic species were measured. The second most abundant isotopic species <sup>41</sup>K<sup>19</sup>F comprises 6.9% of a natural sample and absorption features due to this species were too weak to observe. No measurable absorption features, beyond those attributable to <sup>39</sup>K<sup>19</sup>F, were observed in any of the spectral scans.

The measured wavenumbers for the KF transitions are given in Table IV. These infrared measurements were combined with the microwave measurements given in Refs. (10-12) in a preliminary least-squares analysis based on the Dunham equation (Eq. (1)). As was done for AlF, the lower *J* rotational transitions were corrected for the effects of the hyperfine splittings in order to obtain the hypothetical unsplit center frequency. This was done using the quadrupole constants determined by Van Wachem and Dymanus (21). Each datum in this analysis was weighted by the inverse square of its estimated uncertainty. The constants resulting from this analysis are given in the first column of Table V.

In the same manner as for AlF, the Dunham  $a_i$  constants for KF were determined directly from a nonlinear least-squares fit described below and are given in Table III. These potential constants were then used to determine the values of the constants  $Y_{12}$ ,  $Y_{03}$ , and  $Y_{13}$  and the frequencies were corrected for the effects of these constants. Fixing the values of these constants was necessary since they could not

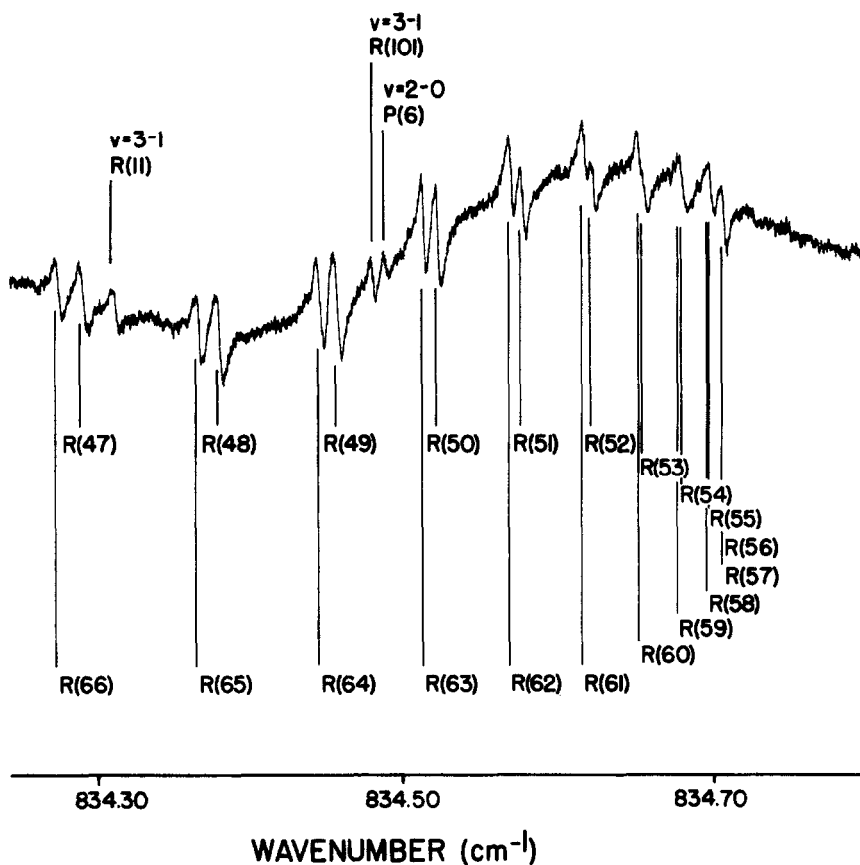


FIG. 1. The first-derivative spectrum of the  $R$ -branch bandhead of the  $^{39}\text{K}^{19}\text{F}$   $v=4-2$  band near  $834.7\text{ cm}^{-1}$ . The spectrum was taken at a temperature of about  $1230\text{ K}$ .

be determined with sufficient accuracy by fitting the data to Eq. (1). Including these constants, however, made very little difference in the values determined for the other  $Y_{ij}$  constants.

In a preliminary fit in which both  $Y_{12}$  and  $Y_{22}$  were allowed to float, we were surprised to discover that  $Y_{22}$  is determined with a precision similar to that for  $Y_{12}$ . This is because  $Y_{22}$  is nearly the same size as  $Y_{12}$  even though it has a higher-order vibrational dependence and therefore would ordinarily be expected to have a value closer to 0.05 times that of  $Y_{12}$ . This experimental observation has been verified by calculating the values of  $Y_{12}$  and  $Y_{22}$  from the Dunham  $a_i$  constants.

#### IV. FITTING THE DATA DIRECTLY TO THE DUNHAM POTENTIAL

The observed transitions also have been fit directly by Dunham's potential constants, the  $a_i$ 's of Dunham's paper (20). This was done partly because of the impressive accuracy of the values of  $Y_{10}$  and  $Y_{20}$  calculated in Refs. (5) and (11) from the potential constants determined from rotational  $Y_{ij}$  terms only. The good agree-

TABLE IV

Observed  $\Delta\nu = 2$  Transitions of Potassium Fluoride ( $^{39}\text{K}^{19}\text{F}$ )

$\nu' - \nu''$	ROT. TRANS	OBSERVED(UNC) <sup>a</sup> ( $\text{cm}^{-1}$ ) <sup>b</sup>	0-C <sup>c</sup> $\times 10^5$ ( $\text{cm}^{-1}$ )
2 - 0	P(6)	834.48707 (50)	57
2 - 0	P(5)	835.09029 (50)	13
2 - 0	R(9)	843.03425 (67)	-33
2 - 0	R(10)	843.48910 (83)	-57
2 - 0	R(24)	848.87032 (50)	2
2 - 0	R(25)	849.18310 (50)	-32
2 - 0	R(36)	851.99448 (50)	-18
2 - 0	R(37)	852.19209 (67)	-30
2 - 0	R(38)	852.38075 (67)	34
2 - 0	R(49)	853.80547 (50)	-47
2 - 0	R(50)	853.87638 (50)	-42
2 - 0	R(51)	853.93799 (50)	15
2 - 0	R(52)	853.98936 (50)	33
2 - 0	R(53)	854.02986 (50)	-51
2 - 0	R(54)	854.06218 (50)	35
2 - 0	R(59)	854.07079 (50)	3
2 - 0	R(60)	854.04293 (50)	15
2 - 0	R(61)	854.00517 (50)	31
2 - 0	R(62)	853.95717 (50)	19
2 - 0	R(63)	853.89923 (50)	8
2 - 0	R(64)	853.83089 (50)	-45
2 - 0	R(75)	852.42418 (67)	35
2 - 0	R(76)	852.23565 (67)	19
2 - 0	R(77)	852.03714 (50)	17
2 - 0	R(89)	848.86278 (67)	35
2 - 0	R(103)	843.29053 (83)	-203
3 - 1	R(8)	832.95668 (50)	-58
3 - 1	R(11)	834.31008 (50)	-33
3 - 1	R(12)	834.74325 (50)	44
3 - 1	R(13)	835.16581 (50)	-4
3 - 1	R(14)	835.58036 (50)	84
3 - 1	R(34)	841.86941 (50)	-26
3 - 1	R(35)	842.08499 (67)	85
3 - 1	R(39)	842.84502 (100)	-80
3 - 1	R(40)	843.01223 (200)	11
3 - 1	R(42)	843.31574 (83)	-1
3 - 1	R(43)	843.45357 (83)	54
3 - 1	R(70)	843.45951 (133)	83
3 - 1	R(71)	843.32122 (133)	84
3 - 1	R(73)	843.01223 (200)	-152
3 - 1	R(74)	842.84502 (100)	-40
3 - 1	R(78)	842.07195 (83)	21

ment found in other instances where observed values of  $Y_{ij}$  constants can be compared with those calculated from independently determined  $a_i$  constants also gave us confidence that a better way of fitting the data might be in terms of the Dunham  $a_i$  constants.

One problem that occurs with the usual technique of fitting the Dunham  $Y_{ij}$  constants is that some of them cannot be determined directly, but should be calculated from the Dunham  $a_i$  constants which are in turn calculated from the determinable  $Y_{ij}$  constants. Furthermore, fitting the data in terms of the Dunham  $Y_{ij}$  constants completely ignores the physics involved. Fitting in terms of the Dunham potential constants (the  $a_i$ 's) takes into account the relationship that exists among the  $Y_{ij}$  terms due to the physics of a vibrating rotor in a potential well, albeit in an approximate fashion due to the truncated power series that must be used to represent the potential function.

TABLE IV—Continued

$\nu' - \nu''$	ROT. TRANS.	OBSERVED(UNC) <sup>a</sup> ( $\text{cm}^{-1}$ ) <sup>b</sup>	0-c <sup>c</sup> $\times 10^5$ ( $\text{cm}^{-1}$ )
3 - 1	R(79)	841.85350(100)	32
3 - 1	R(101)	834.47796(50)	3
4 - 2	R(37)	832.88910(50)	-59
4 - 2	R(38)	833.07279(50)	-14
4 - 2	R(39)	833.24755(100)	95
4 - 2	R(41)	833.56527(83)	14
4 - 2	R(42)	833.71183(83)	185
4 - 2	R(44)	833.97021(50)	-58
4 - 2	R(45)	834.08649(50)	-24
4 - 2	R(47)	834.28923(50)	-39
4 - 2	R(48)	834.37656(50)	0
4 - 2	R(49)	834.45368(50)	-12
4 - 2	R(50)	834.52153(50)	19
4 - 2	R(51)	834.57933(50)	16
4 - 2	R(52)	834.62757(100)	29
4 - 2	R(53)	834.66629(100)	64
4 - 2	R(60)	834.66126(100)	38
4 - 2	R(61)	834.62080(100)	-22
4 - 2	R(62)	834.57143(50)	11
4 - 2	R(63)	834.51209(50)	29
4 - 2	R(64)	834.44231(50)	-11
4 - 2	R(65)	834.36288(50)	-30
4 - 2	R(66)	834.27386(50)	-23
4 - 2	R(68)	834.06685(83)	61
4 - 2	R(69)	833.94720(50)	-28
4 - 2	R(71)	833.68115(83)	94
4 - 2	R(72)	833.53181(83)	12
4 - 2	R(74)	833.20532(100)	49
4 - 2	R(75)	833.02643(50)	-3

<sup>a</sup> The estimated uncertainties in the last digits of the measured values are given in parentheses following each value for the observed wavenumber.

<sup>b</sup> To convert to frequency units use the speed of light:  
 $c=299792.458$  km/s.

<sup>c</sup> The last column gives the differences between the observed wavenumbers and the wavenumbers calculated using the Dunham potential constants given in Table III.

Since the transition frequencies are not expressible as a linear function of the  $a_i$ 's, it is necessary to use a nonlinear least-squares procedure to determine the  $a_i$ 's directly from the transition frequencies. To make such a fit we have written a computer program based on Eqs. (15) in Dunham's paper (20). This program effectively substitutes into Eq. (1) Dunham's expressions for the  $Y_{ij}$  constants in terms of  $B_e$ ,  $\omega_e$ , and the  $a_i$  potential constants. One then has an expression of the form

$$\nu_{\text{obs}} = f(B_e, \omega_e, a_1, a_2, a_3, a_4, a_5, a_6), \quad (2)$$

where  $f(B_e, \omega_e, a_1, a_2, a_3, a_4, a_5, a_6)$  is a nonlinear function of the potential constants  $B_e$ ,  $\omega_e$ ,  $a_1$ , etc.

The same infrared and microwave measurements and weights were used in the nonlinear fits as were used in the linear fits described in the preceding section.

Table III contains the values of the Dunham  $a_i$  constants found from this direct fit to the observed transitions. The second columns in Tables II and V give the

TABLE V  
Dunham Rovibrational Constants for  $^{39}\text{K}^{19}\text{F}$

	This work Fit of $Y_{ij}$	This work <sup>a</sup> Fit of $a_i$	Veazey and Gordy - Ref. (11)
$Y_{10}(\text{cm}^{-1})^b$	426.26119(84) <sup>c</sup>	426.26207(70)	426.04(48)
$Y_{20}(\text{cm}^{-1})^b$	-2.449513(400)	-2.450261(415)	-2.43(18)
$Y_{30}(\text{cm}^{-1})^b$	0.0093447(564)	0.009587(111)	-
$Y_{40}(\text{cm}^{-1})^b$	-	-0.0000250(104)	-
$Y_{01}(\text{MHz})$	8392.31658(193)	8392.31241(315)	8392.313(10)
$Y_{11}(\text{MHz})$	-70.01043(290)	-69.99920(709)	-69.999(16)
$Y_{21}(\text{kHz})$	211.57(75)	205.06(343)	207(4)
$Y_{31}(\text{kHz})$	-	0.794(344)	-
$Y_{02}(\text{kHz})$	-14.4860(149)	-14.478014(70)	-14.493(32)
$Y_{12}(\text{Hz})$	[1.9] <sup>d</sup>	1.914(160)	7(50)
$Y_{22}(\text{Hz})$	1.118(74)	1.199(117)	-
$Y_{03}(\text{mHz})$	[-2.9]	-2.9163(53)	[-2.90(8)]
$Y_{13}(\text{mHz})$	[0.19]	0.1892(94)	-
$Y_{04}(\mu\text{Hz})$	-	-0.021482(58)	-
rms dev. of infrared measurements	0.00057 $\text{cm}^{-1}$	0.00055 $\text{cm}^{-1}$	

<sup>a</sup> Calculated from the  $a_i$  values given in Table III.

<sup>b</sup> To convert between wavenumber units and frequency units use the velocity of light  $c=299792.458$  km/s.

<sup>c</sup> The uncertainty in the last digits (twice the estimated standard error) is given in parentheses following each value.

<sup>d</sup> For the least squares fit of the data the values of  $Y_{12}$ ,  $Y_{03}$ , and  $Y_{13}$  were fixed at the values calculated from the  $a_i$  values given in Table III.

values for the  $Y_{ij}$  constants calculated from these  $a_i$  constants. Table III also gives the values for  $\omega_e$  and  $B_e$  since they are required in addition to the  $a_i$  constants in order to fit the observed transitions. The columns giving the observed minus calculated values in Tables I and IV are based on the transition frequencies calculated from the  $Y_{ij}$ 's that were calculated from the constants given in Table III.

The transitions were fit to three potential functions, one that was truncated at  $a_4$ , one truncated at  $a_5$ , and one truncated at  $a_6$ . For KF all three potential functions were nearly equally good at fitting the data and gave nearly the same values for the  $Y_{ij}$  constants. Since the value of  $a_6$  was less than three times its estimated uncertainty, the fit through  $a_5$  was assumed to represent the best potential function. This fit involving seven variables gave a standard deviation comparable to that obtained from a fit of eight Dunham  $Y_{ij}$  variables (and three calculated  $Y_{ij}$  constants).

For AIF the potential function that included the  $a_6$  term seemed to be necessary

to obtain the best fit. Fewer terms seem to be needed for KF because the magnitude of the successively higher potential constants is getting smaller for KF whereas their magnitude is getting larger for AlF. For AlF only 8 potential function variables were needed to give the same standard deviation for the fit as was obtained fitting 11  $Y_{ij}$  variables.

The uncertainties in the  $Y_{ij}$  values determined from the potential function constants were nearly the same as the uncertainties found in the direct fit of the  $Y_{ij}$ 's when the direct fit gave well-determined values. On the other hand, when the  $Y_{ij}$  values could not be determined or were poorly determined from the direct fit with Eq. (1), in many cases they could still be determined quite well from the potential constants. One must be careful to remember, however, that the calculated uncertainties in the  $Y_{ij}$  values determined from the potential constants do not take into account the degree to which the truncated potential function fails to agree with reality.

The  $\omega_e$  and  $B_e$  values reported here are based on Dunham's original treatment, consequently only the Dunham corrections have been made. Watson (22, 23) has shown that more corrections are necessary to obtain a true equilibrium bond distance ( $r_e$ ) that is invariant with isotopic substitution. Nevertheless, we believe that with the usual mass relationships for  $\omega_e$  and  $B_e$  one could use the constants in Table III to calculate transitions for any other isotopic species (i.e., for  $^{41}\text{K}^{19}\text{F}$ ) with accuracies comparable to the accuracy of the present infrared measurements. Such calculations are being tested with SnO and LiF data and will be reported elsewhere.

One should also note that Dunham's equations are not even complete through  $a_6$  because some terms smaller by  $B_e^2/\omega_e^2$  have been left out of the expressions for  $Y_{30}$ ,  $Y_{40}$ ,  $Y_{21}$ ,  $Y_{31}$ ,  $Y_{22}$ ,  $Y_{03}$ ,  $Y_{13}$ , and  $Y_{04}$ . For more extensive or more accurate measurements it may be necessary to extend Dunham's expressions to include these terms and/or to include  $a_7$  and higher-order terms in the potential function. Such an extension has already been made by Sandeman (24) although his expressions are awkward to use since they use a new set of variables that are not linearly related to the  $a$ 's.

We would also like to point out that Niay *et al.* (25) have similarly fit the spectrum of HBr directly in terms of the Dunham potential constants. They have found it necessary to extend Dunham's treatment to include  $a_7$  and  $a_8$ .

#### CONCLUSION

For the first time high-resolution, high-temperature gas-phase infrared measurements have been made on AlF and KF. These measurements and microwave measurements made elsewhere have been analyzed with a nonlinear least-squares program to obtain values for  $B_e$ ,  $\omega_e$ , and the Dunham potential constants  $a_1$ ,  $a_2$ ,  $a_3$ ,  $a_4$ ,  $a_5$ , and  $a_6$ . In a comparison with the usual procedure of fitting to a set of Dunham  $Y_{ij}$  constants, it is shown that fewer potential constants are needed to give a comparable fit to the observed transition frequencies.

We believe that fitting the rovibrational transition data directly to the Dunham potential constants has several advantages over fitting the data directly to the Dunham  $Y_{ij}$  constants. (1) Since fewer constants are needed, the Dunham potential

constants can be used to calculate unobserved transitions with greater reliability. It is well known that both interpolation and extrapolation calculations can deviate more quickly from "true values" when high-order polynomials are used to fit the data than when low-order polynomials are used. (2) Fitting the rovibrational transitions to the Dunham potential function utilizes our understanding of the physical processes involved much more than fitting to a power series in  $v$  and  $J$ . Such a fit to the potential function provides a theoretical model in which the physically significant correlations between different  $Y_{ij}$  constants are preserved. On the other hand, fitting directly to a series of  $Y_{ij}$  constants is tantamount to assuming that these constants are not correlated. (3) The truncation of the potential constants is more natural and more easily chosen since, for most data collections that we have observed, each succeeding higher-order potential constant has a greater uncertainty and makes a smaller contribution to the observables. (4) The isotope shifts are more exactly calculated from the potential function since it takes into account some of the correction factors that are smaller than the  $Y_{ij}$  terms by a factor of  $B_e^2/\omega_e^2$ .

The Dunham  $Y_{10}$  constants given in Table V and the variance-covariance matrix given by the least-squares fit of the data have been used to calculate the band centers for the three  $\Delta v = 2$  bands of KF measured in this work with the results  $\nu_0(2-0) = 837.97020 \pm 0.00024 \text{ cm}^{-1}$ ,  $\nu_0(3-1) = 828.39659 \pm 0.00028 \text{ cm}^{-1}$ , and  $\nu_0(4-2) = 818.93503 \pm 0.00048 \text{ cm}^{-1}$ . Since the much stronger  $\Delta v = 1$  transitions may be of greater interest, we have also calculated the following band centers  $\nu_0(1-0) = 421.39258 \pm 0.00020 \text{ cm}^{-1}$ ,  $\nu_0(2-1) = 416.57762 \pm 0.00010 \text{ cm}^{-1}$ , and  $\nu_0(3-2) = 411.81897 \pm 0.00020 \text{ cm}^{-1}$ . The uncertainties given for all these band centers are twice the statistically estimated standard error. The 1-0 band center is slightly higher in the gas phase than the value of  $397 \text{ cm}^{-1}$  found by Ismail *et al.* (15) for KF when trapped in a solid argon matrix at low temperatures.

The band centers for the three vibrational transitions of AlF that we measured are:  $\nu_0(1-0) = 792.6882 \pm 0.0004 \text{ cm}^{-1}$ ,  $\nu_0(2-1) = 783.1633 \pm 0.0004 \text{ cm}^{-1}$ , and  $\nu_0(3-2) = 773.7534 \pm 0.0007 \text{ cm}^{-1}$ . According to Snelson (9), the 1-0 band is slightly lower in frequency in a low-temperature solid argon matrix,  $776 \text{ cm}^{-1}$ .

#### ACKNOWLEDGMENT

The authors are indebted to Wm. Bruce Olson, who built the diode laser spectrometer and who maintains it in excellent working condition. Dr. Olson's modifications to obtain first-derivative spectra with high sensitivity were essential for observing the KF transitions, which were all very weak.

RECEIVED: May 6, 1982

#### REFERENCES

1. K. P. HUBER AND G. HERZBERG, "Molecular Spectra and Molecular Structure IV. Constants of Diatomic Molecules," Van Nostrand-Reinhold, New York, 1979.
2. R. F. BARROW, I. KOPP, AND C. MALMBERG, *Phys. Scripta* **10**, 86-102 (1974).
3. D. R. LIDE, *J. Chem. Phys.* **38**, 2027 (1963).
4. D. R. LIDE, *J. Chem. Phys.* **42**, 1013-1018 (1965).
5. F. C. WYSE, W. GORDY, AND E. F. PEARSON, *J. Chem. Phys.* **52**, 3887-3889 (1970).
6. J. HOEFT, F. J. LOVAS, E. TIEMANN, AND T. TORRING, *Z. Naturforsch. A* **25**, 1029-1035 (1970).

7. R. HONERJAGER AND R. TISCHER, *Z. Naturforsch. A* **29**, 342-345 (1974).
8. W. W. RICE AND R. J. JENSEN, *Appl. Phys. Lett.* **22**, 67-68 (1973).
9. A. SNELSON, *J. Phys. Chem.* **71**, 3202-3207 (1967).
10. G. W. GREEN AND H. LEW, *Canad. J. Phys.* **38**, 482-494 (1960).
11. S. E. VEAZEY AND W. GORDY, *Phys. Rev. A* **138**, 1303-1311 (1965).
12. H. DIJKERMAN, W. FLEGEL, G. GRAFF, AND B. MONTER, *Z. Naturforsch. A* **27**, 100-110 (1972).
13. R. K. RITCHIE AND H. LEW, *Canad. J. Phys.* **42**, 43-52 (1964).
14. V. I. BAIKOV AND K. P. VASILEVSKII, *Opt. Spektrosk.* **22**, 364-372 (1967); *Opt. Spectrosc.* **22**, 198-202 (1967).
15. Z. K. ISMAIL, R. H. HAUGE, AND J. L. MARGRAVE, *J. Inorg. Nucl. Chem.* **35**, 3201-3206 (1973).
16. F. J. LOVAS, A. G. MAKI, AND W. B. OLSON, *J. Mol. Spectrosc.* **87**, 449-458 (1981).
17. J. S. WELLS, F. R. PETERSEN, A. G. MAKI, AND D. J. SUKLE, *Appl. Opt.* **20**, 1676-1684 (1981); **20**, 2874 (1981).
18. J. S. WELLS, F. R. PETERSEN, A. G. MAKI, AND D. J. SUKLE, *J. Mol. Spectrosc.* **89**, 421-429 (1981).
19. A. G. MAKI AND F. J. LOVAS, *J. Mol. Spectrosc.* **85**, 368-374 (1981).
20. J. L. DUNHAM, *Phys. Rev.* **41**, 721-731 (1932).
21. R. VAN WACHEM AND A. DYMANUS, *J. Chem. Phys.* **46**, 3749-3756 (1967).
22. J. K. G. WATSON, *J. Mol. Spectrosc.* **45**, 99-113 (1973).
23. J. K. G. WATSON, *J. Mol. Spectrosc.* **80**, 411-421 (1980).
24. I. SANDEMAN, *Proc. Roy. Soc. Edinburgh* **60**, 210-223 (1940).
25. P. NIAY, P. BERNAGE, C. COQUANT, AND A. FAYT, *Canad. J. Phys.* **55**, 1829-1834 (1977).